Flow Field in Swirl-Type Tubular Flame Burner*

Yuyin ZHANG**, Daisuke SHIMOKURI**, Yoshihisa MUKAE** and Satoru ISHIZUKA**

The flow field in swirl-type tubular flame burners was measured using a Particle Imaging Velocimetry (PIV) system with an easily controlled kerosene droplet tracer generator. Through characterization of the flow field in two burners with different swirl numbers, it was found that the flow is an axisymmetric vortex flow. The tangential component of the velocity is zero at the tube center, and increases proportionally with radius at first, and then falls slowly in a radial direction. The gradient of the tangential component near the vortex center depends significantly on the swirl number and the flow rate. The vortex center oscillates around the tube center in a roughly circular area, and this precession is significantly sensitive to the swirl number. The radius of the precession area shrinks as the swirl number increases. The radial distributions of the axial velocity take a plateau-shape for the weak swirl burner (swirl number $S = 0.21$), whereas they take an "M" shape for the strong swirl burner ($S = 0.78$) with reverse flow in the vicinity of the burner axis. The occurrence of the axial reverse flow is dominated by the swirl number, and is affected by the flow rate as well. Finally, a comparison was made between the swirl numbers calculated with the measured velocity profiles in a cross section and those calculated from the input angular momentum.

***Key Words*:** Burner, Flow Measurements, Swirling Flow, Vortex

1. Introduction

In the last decade, swirl type tubular flame, which can be easily established in a tube where a fuel/air mixture is injected tangentially with the exhaust gas exiting axially, have attracted the interest of many researchers [(1)–(10)], because this type of flame has excellent combustion characteristics such as heat loss, aerodynamic stability, and similarity. Therefore, a further attempt has been made recently to use the tubular flame for a practical combustor, and a prototype burner, in which the combustible mixture is tangentially injected, has been proposed [(11)–(14)].

However, the flow field in the tubular flame burner has not yet been systematically investigated. As is well known, swirl flows are widely used for combustion in gas turbine engines or in industrial furnaces [(15)–(18)], which yield turbulent combustion within bulk reaction zones. The tubular flame burner also uses a swirl flow, but it yields laminar combustion with a tubular flame, the diameter of which is constant in the longitudinal direction and the flame structure is consistently laminar [(11)–(14)]. Thus, with a view towards understanding such a tubular flame, it is important to identify the flow characteristics of the tubular flame burner.

Kobayashi and Kitano [(19)] measured the axial and radial velocity profiles for a nonswirl tubular flame burner using LDA. For a swirl-type tubular flame burner, Ishizuka [(2)] adopted a hotwire anemometry to obtain the tangential velocity profiles under a cold flow condition. However, as a vortex flow is extremely sensitive to disturbances created by even a tiny probe and the signal is difficult to adjust to zero at the vortex axis due to the so-called zero floating of the hotwire system, the hotwire measurements were unconvincing. On the other hand, LDA measurements of a turbulent vortex flow in a cylinder, which was geometrically similar to the burner used in this study, have been reported [(20)], but the fluid used was water. To date, therefore, reliable measurements of flow structure and velocity profiles in the swirl-type tubular flame burner have been lacking.

This situation is now changing due to progress in laser diagnostics. The PIV technique should be mentioned here as it is advantageous over LDA technique in providing instantaneous velocity profiles of a flow field. For a swirl-type tubular flame burner, an instantaneous velocity profile is of particular importance because a vortex flow typically has irregular variation in the velocity distributions due to

* Received 20th May, 2005 (No. 05-4046)

** Department of Mechanical System Engineering, Hiroshima University, 1–4–1 Kagamiyama, Higashi-Hiroshima 739–8527, Japan.
E-mail: yyzhang@mec.hiroshima-u.ac.jp

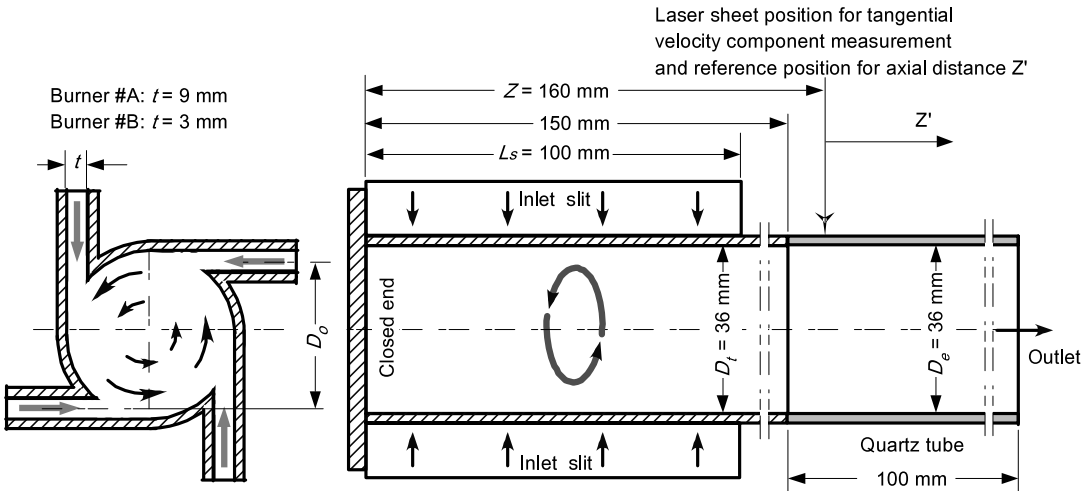

Fig. 1 Configuration of swirl-type tubular flame burner

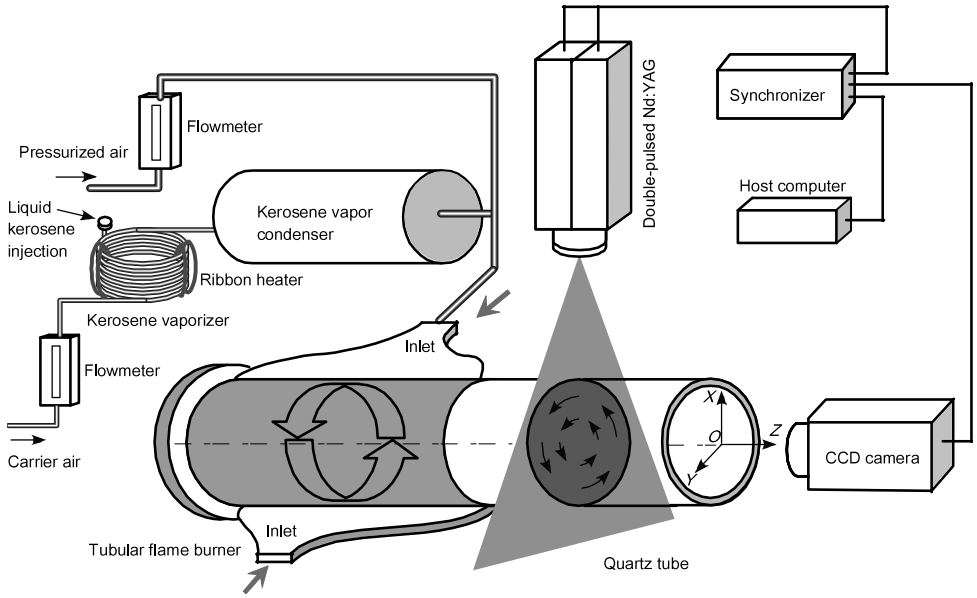

Fig. 2 Optical arrangement of PIV system and the kerosene droplet tracer supplying apparatus

precession of the vortex center. Thus, the PIV technique is more applicable to characterization of the flow field in the swirl-type tubular flame burner if the effect of centrifugal force on the tracers is adequately minimized so that the tracers follow the flow even in a strong swirling flow.

In this study a well-controlled kerosene droplet tracer supplying system was built for the PIV system to minimize the effect of centrifugal force on tracer particles thus facilitating measurements of a strong swirl flow. Using this PIV technique, the flow fields in the swirl-type tubular flame burner were characterized by determining the tangential and axial velocity profiles under cold flow conditions, and the effects of the swirl number and the inflow velocity on the aerodynamics were clarified.

2. Experiments

2.1 Tubular flame burner

A schematic drawing of the swirl-type tubular flame burner is shown in Fig. 1. Cold air is introduced tangentially from four slits and then exits through the open end, while the other end is closed. A swirling flow forms in the tube. The inlet slit length L_s is 100 mm, and the tube diameter D_t is 36 mm. For examining the effect of swirl strength, two burners with different slit widths, t = 9 mm (called burner #A) and 3 mm (called burner #B), were designed.

The so-called swirl number is the most commonly accepted measure of swirl strength, the definition of which was given by Beer and Chigier [15]. According to this definition, the swirl number should, if possible, be calculated from measured velocity and pressure profiles as

$$S \equiv \frac{G_w}{RG_A} = \frac{2\pi \int_0^R \rho W U r^2 dr}{2\pi R \int_0^R \rho U^2 r dr + 2\pi R \int_0^R p r dr}, \qquad (1)$$

where G_w and G_A are the angular and axial momenta, and R, ρ, W, U, and p are the radius of the burner exit, the

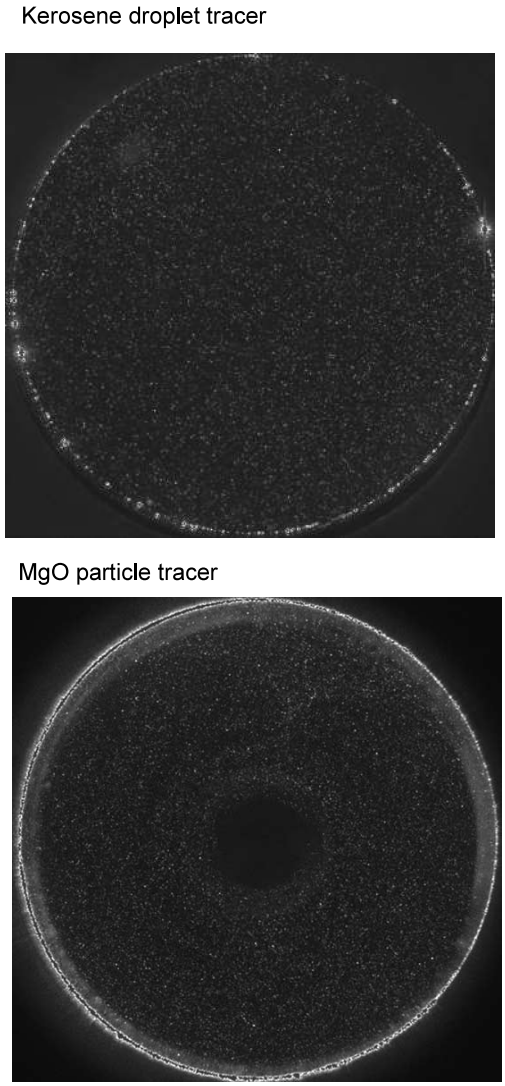

Fig. 3 Images of different PIV tracers in strong vortex flows in cross section $Z = 160$ mm ($S = 3.0$, $Q = 160$ L/min)

fluid density, the tangential and axial components of the velocity, and the static pressure in a cross section of the burner, respectively.

Since it is usually deficient in the detailed experimental data of velocity profiles for a swirl burner or a cyclone combustor, the swirl number has often been defined on the basis of input and exit parameters [1),(16),(17)] as follows:

$$S \equiv \frac{G_w}{RG_A} \approx \frac{Input\ Angular\ Momentum}{D_e/2 \times Exit\ Axial\ Momentum} = \frac{\pi D_e D_o}{4A_T}, \quad (2)$$

where D_o is the diameter of the main section of a swirl burner, D_e is the exit throat diameter, and A_T is the total sectional area of the tangential inlet slits. For a tubular flame burner with N tangential slit(s), the swirl number S can be calculated as

$$S \approx \frac{\pi D_o D_e}{4NL_s t}. \quad (3)$$

Following the previous study [16] in which a swirl burner with four slits was used, D_o is determined by subtracting

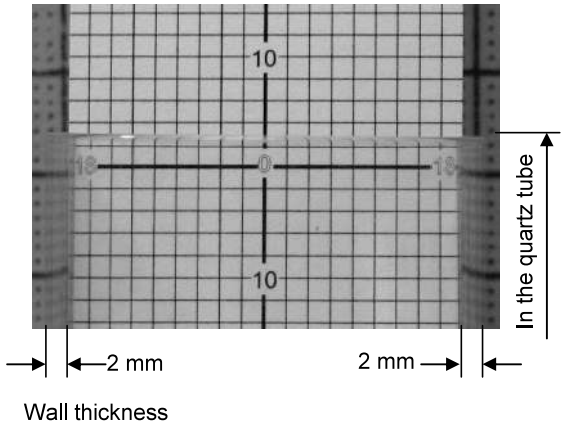

Fig. 4 Image distortion due to refraction of cylindrical lens effect of quartz tube wall.

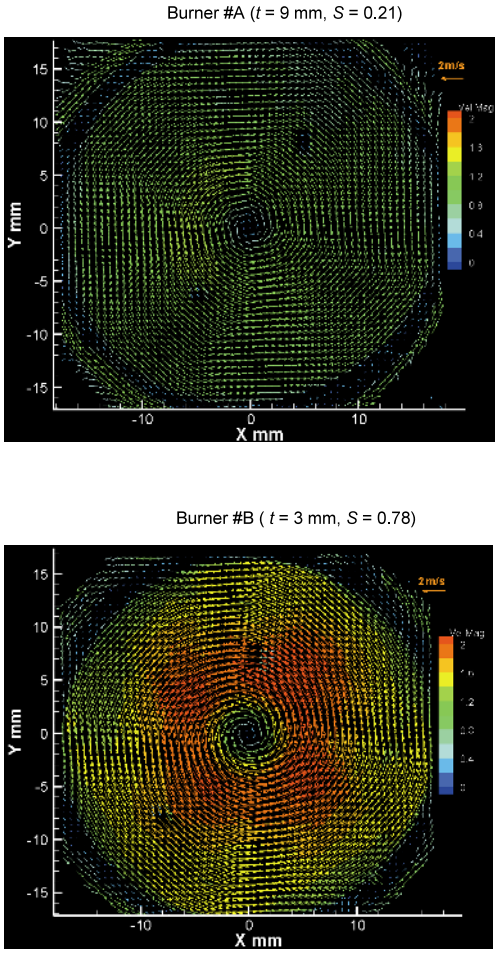

Fig. 5 Mean velocity profiles in cross section perpendicular to tube axis ($Q = 80$ L/min)

the slit width from the burner diameter, i.e., $D_o = D_t - t$ (refer to Fig. 1). Thus, the swirl numbers S can be easily worked out to be 0.21 and 0.78, respectively, for burners #A ($t = 9$ mm) and #B ($t = 3$ mm). More discussion about swirl number can be found in the next section.

The vortex flow in the two burners was examined at flow rates of $Q = 40$, 80, 120 and 160 L/min in this study.

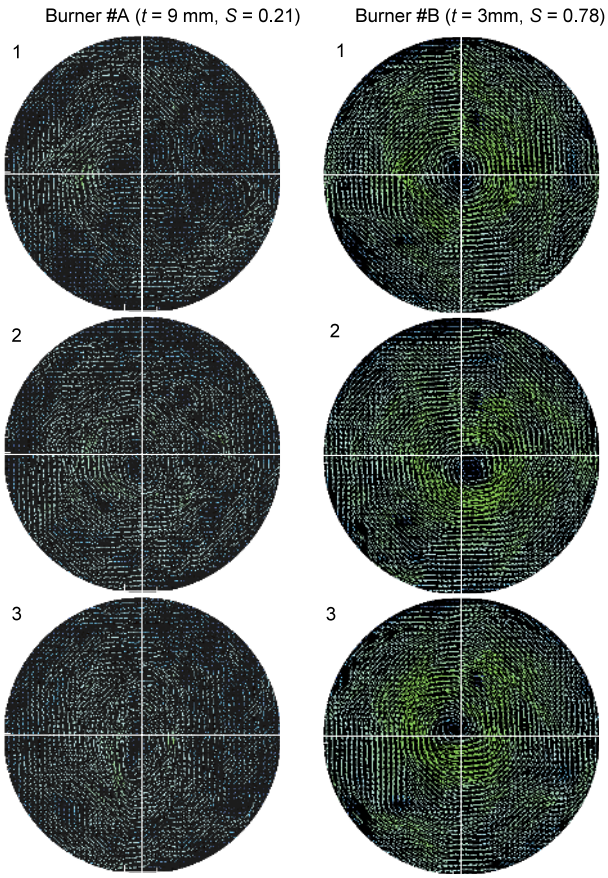

Fig. 6 Instantaneous vector profiles indicating vortex recession cross section $Z = 160$ mm ($Q = 80$ L/min, time interval: 1/15 sec, sequence: $1 \rightarrow 2 \rightarrow 3$)

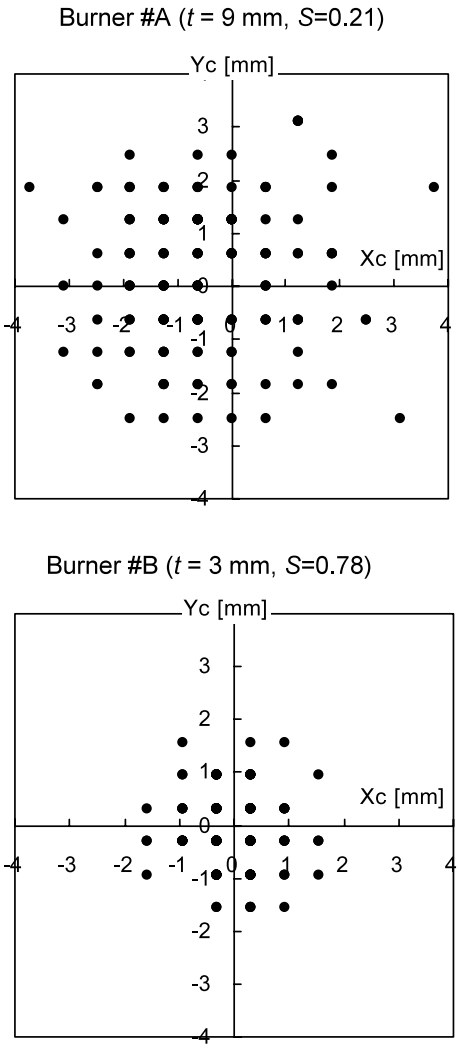

Fig. 7 Trajectory of vortex center (Xc, Yc) obtained from vector profiles in cross section $Z = 160$ mm ($Q = 80$ L/min)

2.2 PIV measurements

Figure 2 shows the optical arrangement of the PIV system equipped with the proposed size-controllable droplet tracer generator for the measurement of vortex flow in the tubular flame burners. The PIV system consists of a high-resolution CCD camera (TSI, $1\,280 \times 1\,024$ pixels, 10-bit grayscale), a double-pulsed Nd:YAG laser (120 mJ/pulse, 15 Hz), a host computer, and a synchronizer. Double-pulsed laser sheets are directed to the quartz tube, which is a chimney of the tubular flame burner, perpendicularly with respect to the tube axis when measuring the tangential velocity component, while the sheets pass through the tube axis when measuring the axial component.

A strong vortex flow usually results in a significant centrifugal force on the tracers in it. This centrifugal force always keeps the tracers out of the region near the vortex axis. To measure a strong vortex flow, one of the most important requirements is to generate tracers of desirable size and scatter them uniformly in the flow field of interest. A kerosene droplet tracer generator, therefore, was designed in this study (see Fig. 2). It consists of a tank in which kerosene vapor condenses to droplets, a vaporizer which comprises a coiled copper pipe and an electrical heater with a temperature controller, a syringe for liquid kerosene metering and injection, a thermometer and a flowmeter. The kerosene quantity injected, the temperature of the vaporizer, the time of condensation in the tank and the carrier gas flow rate could be adjusted according to the operating conditions and the requirements for the tracer density and size (diameter). For instance, in the case of strong vortex flow, fine droplets are required; thus, the vaporization temperature should be elevated to a higher degree and the condensation time should be shortened. In contrast, for low flow rate and weak vortex flow conditions, the condensation time should be longer; otherwise the droplets become so small that only smoke can be seen in the burner.

This carefully designed PIV tracer generator greatly facilitates the measurements of even a strong vortex flow in the tubular flame burners because it is capable of providing very uniform and fine droplets (tracer) for almost all operating conditions and, most important, the size and

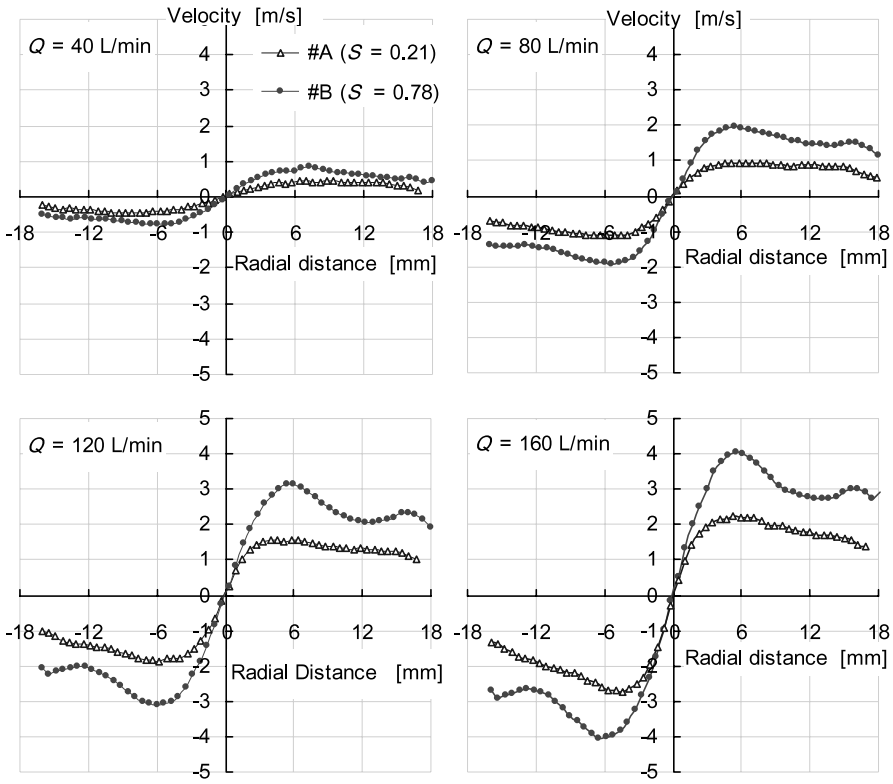

Fig. 8 Radial distributions of tangential velocity component in cross section $Z = 160$ mm. The results are obtained by averaging 200 measurements for each condition.

density of droplets can be easily controlled compared with those of other tracers such as MgO or "microballoon" solid particles. Figure 3 shows an example of PIV images of kerosene droplet tracers compared with that of MgO tracers (~5 μm) in a strong vortex flow. The tracers distribute themselves uniformly in the whole area even in the vortex center in the case of kerosene droplets, whereas there appears a "black hole" due to the absence of MgO particles near the center of the vortex. The latter case will inevitably cause problems in the interpretation of velocity profiles in the vortex center area.

In measuring the axial velocity component distribution, the problem which must be faced is the image distortion due to the light refraction resulting from the cylindrical lens effect of the quartz tube. This has frustrated many researchers' attempts, although some researchers have proposed a complicated arithmetic method for distortion correction. In this study, it has been confirmed (see Fig. 4) that there is no distortion in the axial direction at all, whereas in the radial direction a severe distortion appears near the quartz walls, but it becomes negligible in the vicinity of the tube axis. This indicates that measurements of the axial velocity component in the quartz tube are reliable, but those of the radial component, especially in the area far from the central axis, are underestimated, according to the PIV principle.

3. Results and Discussion

Characterization of the flow field is carried out using two tubular flame burners with different swirl numbers. Taking into account the flow fluctuation, the measurement for each operating condition is implemented 200 times at an interval of 1/15 sec. All mean velocity distributions or mean vector profiles given in the following are obtained by averaging 200 measurements.

3.1 Tangential velocity component

Figure 5 shows the mean velocity vector profiles in a cross section ($Z = 160$ mm) perpendicular to the tube axis of the two burners with different swirl numbers at a flow rate of 80 L/min. The two velocity profiles look similar in shape but differ in magnitude. They represent apparently an axisymmetric vortex flow with the vortex axis located near the tube center. For both burners #A and #B, the velocity is zero at the center, increases along the radial direction at first, and then falls gradually to a value most likely close to the injection velocity at the slit inlet.

Figure 6 demonstrates sequentially the instantaneous velocity vector profiles of the two burners at $Q = 80$ L/min with a crosshair showing the tube geometric center. The time interval between two measurements is 1/15 sec. From these results, the detailed vortex flow structure can be observed. First, a precession phenomenon of the vortex can be seen: the vortex center moves around the tube's geo-

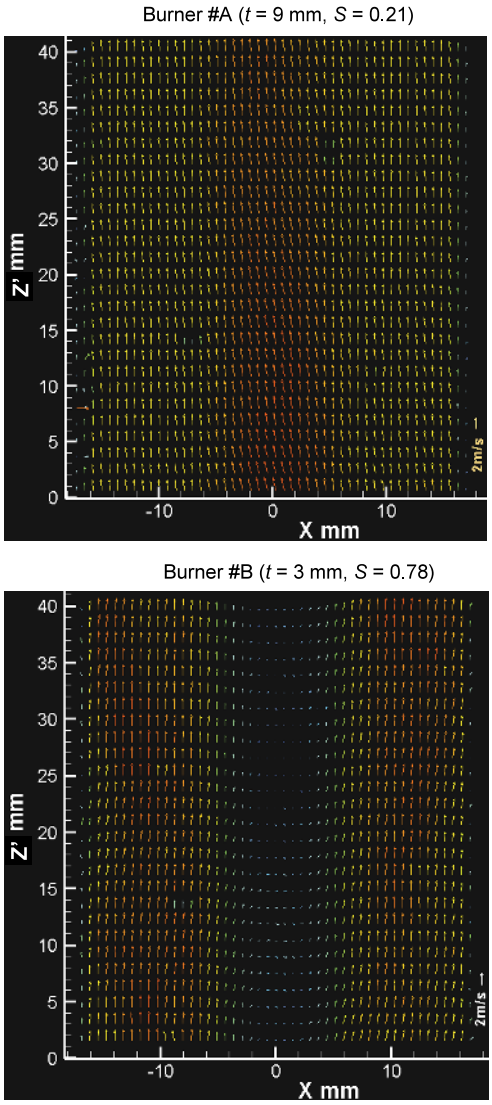

Fig. 9 Mean velocity profiles in plane containing tube axis (Q = 80 L/min). The results are obtained by averaging 200 measurements for each condition. Z' is the axial distance from the reference position in Fig. 1.

metric center, but remains close to it. Second, the vortex mostly maintains in a stable structure or a steady flow pattern, but deformation of the vortex core takes place occasionally, particularly in burner #A (S = 0.21).

The vortex precession can be interpreted as the variation of the vortex center in the X-Y plane. Figure 7 shows the trajectories of the vortex center (Xc, Yc) measured directly from the vector profiles. The results indicate that the vortex center oscillates around the tube center roughly in a circular area. The radius of the precession range is within approximately 4 mm for burner #A (S = 0.21), which is considerably large if compared with the tube radius, R = 18 mm. For burner #B (S = 0.78), however, it decreases to about 2 mm. Thus, it is found that the precession is considerably sensitive to the swirl number. The radius of the precession area shrinks as the swirl number increases.

Figure 8 shows the radial distributions of the tangential component in the two burners at flow rates of 40, 80, 120 and 160 L/min. The data were obtained from the mean velocity vectors in the cross section perpendicular to the tube axis with the vortex axis being aligned to the tube axis. For all the burner and flow rate conditions, the magnitude of the tangential velocity component is zero at the tube center, increases linearly with radius, reaches its peak midway to the tube wall, and then falls slowly as the wall is approached. For burner #B, a small second peak appears near the wall. This second peak was presumably caused by the air injection at the inlet slits. Such a two-peak-profile was also observed by Ishizuka [2] in his hotwire measurements. The gradient of the tangential component near the vortex center depends significantly on the swirl number and the flow rate. A higher swirl number or flow rate leads to an abrupt rise in the tangential velocity near the vortex center.

3.2 Axial velocity component

Figure 9 shows the mean velocity vector profiles in the cross section through the tube axis of burners #A and #B. As mentioned earlier, since there is no image distortion in the axial (Z) direction, the measurements of the axial velocity component are reliable. From Fig. 9, the following results can be obtained. First, the radial component is small compared with the axial one. Second, the vector profiles appear fairly uniform along the tube axis but not in the radial direction. Third, the flow patterns are very different between the two burners. For the weak swirl burner (#A), the flow near the axis goes toward the open end, and the magnitude is slightly larger than that out of the axis; whereas for the stronger swirl burner (#B), the flow near the tube axis is negligible or in the reverse direction towards the closed end, while the flow out of the vicinity of the axis takes a distribution similar to that of the weak swirl burner (#A).

The axial flow fluctuation is illustrated in Fig. 10. The sequential velocity vector profiles were taken at an interval of 1/15 sec. For both burners, the flow is almost stable and straight, but fluctuations do exist especially in the vicinity of the tube axis. This presumably results from the vortex precession [21], which has also proved to be true by the tangential component distributions in this study (see section 3.1).

The difference in the distribution of the axial component between the two burners at flow rates of 40, 80, 120 and 160 L/min is shown in Fig. 11. Generally, for all flow rate conditions of the weak swirl burner (#A), the distribution of the axial velocity takes a plateau shape but the axial velocity decreases gradually as the wall is approached and finally falls rapidly near the wall. In contrast, for the strong swirl burner (#B) the radial distribution of the axial velocity is "M" shaped, i.e., the velocity is close to zero or even negative (a reverse flow occurs) on the tube

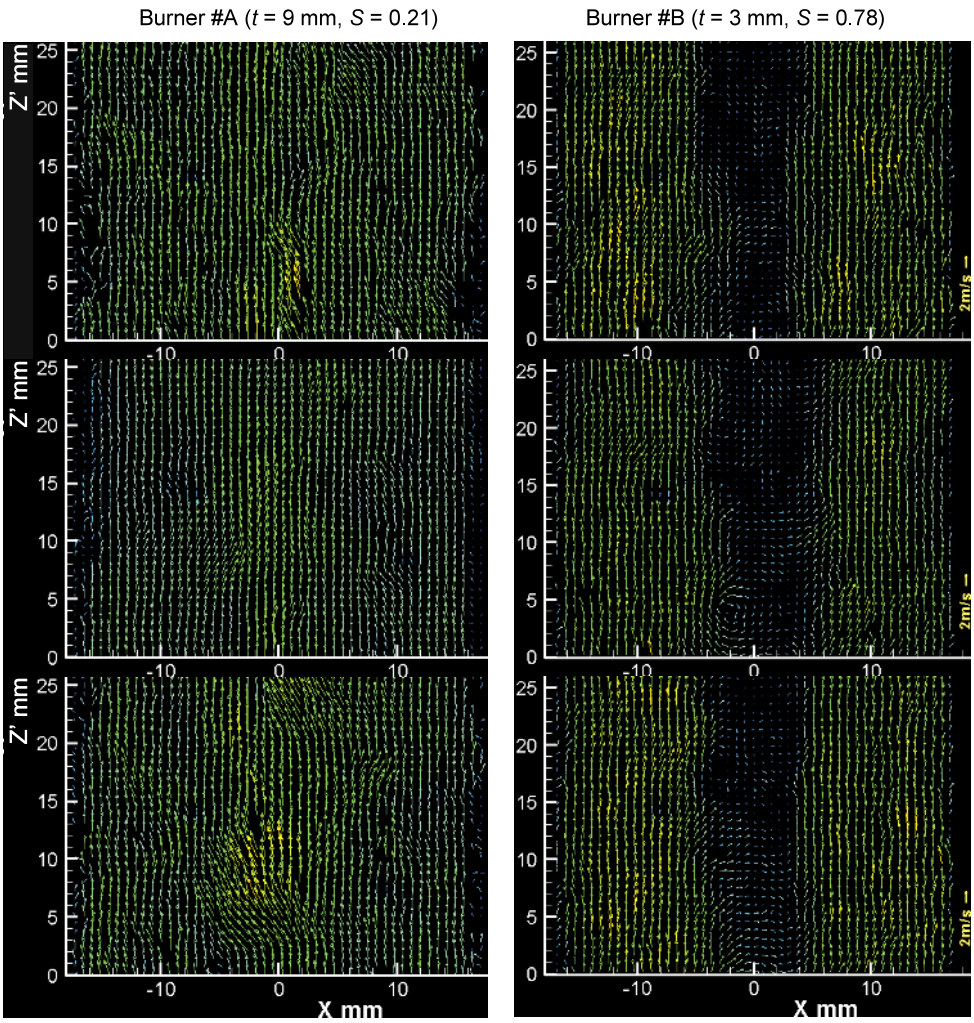

Fig. 10 Instantaneous vector profiles in tube-axis plane indicating flow fluctuation. Z' is the axial distance from the reference position in Fig. 1 (Q = 80 L/min, time interval: 1/15 sec, sequence: from top to bottom).

axis, rises steadily along the radius at first, and then falls abruptly again to a low value near the wall. Furthermore, the magnitude of the reverse flow near the vortex axis increases slightly with flow rate. Thus, the occurrence of the reverse flow in the axial direction is dominated by the swirl number, and to some extent affected by the flow rate as well.

3.3 Swirl number

The swirl number of the two burners is calculated using the exact definition, Eq. (1). For this calculation, the profiles of the tangential and axial components of the velocity measured in the cross section at the axial distance of Z = 160 mm (see Fig. 1) are used, while the term of static pressure in Eq. (1) is omitted. Table 1 gives the results obtained by this calculation and compares them with those calculated with the input angular momentum. It is found that first, the swirl numbers calculated with the velocity profiles are almost unchanged as the flow rate varies from 80 to 160 L/min for both burners, as expected; second, according to the comparison of the swirl numbers calculated with the velocity profiles at Z = 160 mm with those calculated with the input data, the former are approximately 25% greater than the latter for the weak swirl burner (#A) and approximately 30% smaller than the latter for the strong swirl burner (#B). Since a strong swirl flow usually leads to considerable pressure gradients and negative static pressure, neglecting the static pressure term may contribute to this underestimation of the swirl number for burner #B. This discrepancy suggests, nevertheless, the degree to which the swirl number calculated from the input tangential momentum can represent the actual one is worthy of further investigation.

3.4 Accuracy of velocity measurements

To validate the velocity profiles measured in this work, a series of measurements on the axial velocity profiles in the tubular flame burners have also been performed with the PIV system by varying the flow rate. From the velocity profiles measured, the flow rate can be obtained by

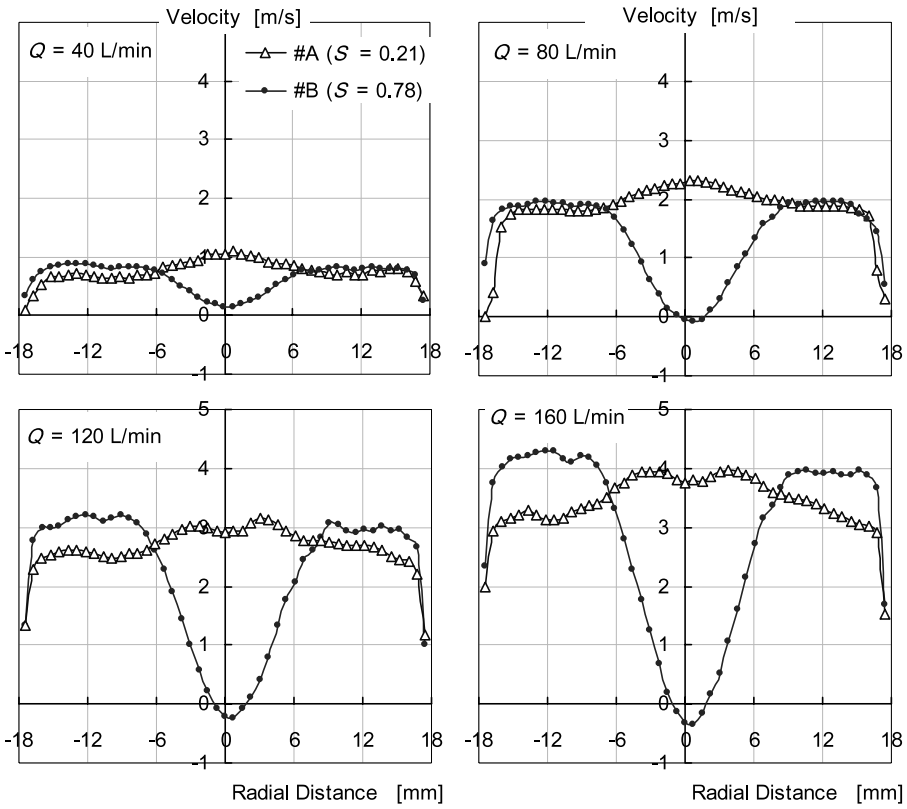

Fig. 11 Radial distributions of axial velocity component. The results are obtained by averaging 200 measurements for each condition.

Table 1 Swirl numbers obtained using different equations.

Calculation method \ Condition	Burner #A (t = 9 mm)		Burner #B (t = 3 mm)	
	80 L/min	160 L/min	80 L/min	160 L/min
input angular momentum	0.21	0.21	0.78	0.78
velocity profiles at Z = 160 mm	0.26	0.28	0.55	0.51

integrating the velocities with the following equation:

$$Q = \sum_{i=1}^{N} 2\pi r_i (r_i - r_{i-1}) U_i, \qquad (4)$$

where $r_0 = 0$ and $r_N = D_e/2$ (N is the number of measurements performed along the tube radius).

The flow rate data obtained from the velocity measurements are plotted in Fig. 12 against those measured with a flowmeter. The plots almost lie on or approach the diagonal line. It is estimated that the relative error in the flow rate calculated from the axial velocity profiles is within approximately 10%. Although the velocity measurements cannot be ensured directly by this error estimation, this finding is quite encouraging; to some degree, it implies that the measurements are reliable.

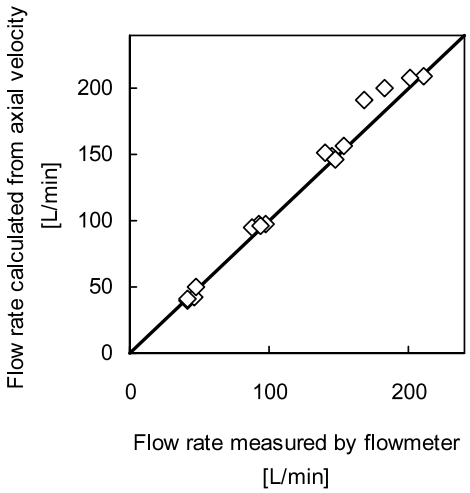

Fig. 12 Flow rate integrated from velocity profiles against that measured with flowmeter.

4. Conclusions

To measure the vortex flow in swirl-type tubular flame burners, a PIV system was established by devising an easily controlled kerosene droplet tracer generator which facilitates strong vortex flow measurements. The measurement accuracy of the PIV system was confirmed to be reliable by comparing the flow rates measured with a flowmeter with those calculated from the axial velocity profiles measured. On the basis of the PIV measurements, characterization of flow field has been performed and the effects of the swirl number and flow rate on the aerodynamics have been examined. The main conclusions are as follows.

(1) Regarding the mean velocity profiles, the tangential component is zero at the tube center, increases propor-

tionally with radius up to a certain point, and then falls slightly as the radial distance further increases. The gradient of the tangential component near the vortex center depends significantly on the swirl number and the flow rate as well.

(2) The vortex center oscillates around the tube center in a roughly circular area. This precession is considerably sensitive to the swirl number. The radius of the precession area shrinks as the swirl number increases.

(3) The profile of the axial velocity takes a plateau shape in the case of the weak swirl burner (S = 0.21), while it takes an "M" shape for the strong swirl burner (S = 0.78) with a reverse flow in the vicinity of the tube axis.

(4) A comparison was made between the swirl numbers calculated with the measured velocity profiles at the cross section Z = 160 mm and those calculated from the input angular momentum. The former is approximately 25% greater than the latter for the weak swirl burner (#A), while it is approximately 30% smaller for the strong swirl burner (#B).

Acknowledgements

This study was financially supported by The New Energy and Industrial Technology Development Organization (NEDO), Japan. The authors also acknowledge with gratitude the assistance of Mr. A. Miyahara in the PIV measurements.

References

(1) Ishizuka, S., On the Behavior of Premixed Flames in a Rotating Flow Field: Establishment of Tubular Flames, Proc. Combust. Inst., Vol.20 (1984), pp.287–294.

(2) Ishizuka, S., Characteristics of Tubular Flames, Prog. Energy Combust. Sci., Vol.19 (1993), pp.187–226.

(3) Takeno, T., Nishioka, M. and Ishizuka, S., A Theoretical Study of Extinction of a Tubular Flame, Combust. Flame, Vol.66 (1986), pp.271–283.

(4) Nishioka, M., Takeno, T. and Ishizuka, S., Effects of Variable Density on a Tubular Flame, Combust. Flame, Vol.73 (1988), pp.287–301.

(5) Kobayashi, H., Kitano, M. and Otsuka, Y., A Study on the Extinction of a Stretched Cylindrical Premixed Flame, Trans. Jpn. Soc. Mech. Eng., (in Japanese), Vol.52, No.483, B (1986), pp.3811–3817.

(6) Libby, P.A., Peters, N. and Williams, F.A., Cylindrical Premixed Laminar Flames, Combust. Flame, Vol.75 (1989), pp.265–280.

(7) Sakai, Y. and Ishizuka, S., Structure of Tubular Flames (1st Report, Structures of the Tubular Flames of Lean Methane/Air Mixtures in a RotatingStretched-Flow Field), Trans. Jpn. Soc. Mech. Eng., (in Japanese), Vol.56, No.524, B (1990), pp.1178–1185.

(8) Sakai, Y. and Ishizuka, S., Structure of Tubular Flames (1st Report, Structures of the Tubular Flames of Lean Methane/Air Mixtures in a Rotating Stretched-Flow Field), JSME Int. J., Ser. II, Vol.34, No.2 (1991), pp.234–241.

(9) Yamamoto, K., Ishizuka, S. and Hirano, T., Effect of Rotation on the Stability and Structure of Tubular Flame, Proc. Combust. Inst., Vol.25 (1994), pp.1399–1406.

(10) Mosbacher, D.M., Wehrmayer, J.A., Pitz, R.W., Sung, C.J. and Byrd, J.L., Experimental and Numerical Investigation of Premixed Tubular Flames, Proc. Combust. Inst., Vol.29 (2002), pp.1479–1486.

(11) Ishizuka, S., Hagiwara, R., Suzuki, M., Nakamura, A. and Hamaguchi, O., Combustion Characteristics of a Tubular Flame Burner, Trans. Jpn. Soc. Mech. Eng., (in Japanese), Vol.65, No.639, B (1999), pp.3845–3852.

(12) Hagiwara, R., Okamoto, M., Ishizuka, S., Kobayashi, H., Nakamura, A. and Suzuki, M., Combustion Characteristics of a Tubular Flame Burner for Methane, Trans. Jpn. Soc. Mech. Eng., (in Japanese), Vol.66, No.652, B (2000), pp.3226–3232.

(13) Ishizuka, S., Suzukawa, Y., Ishioka, M. and Okada, K., A Burner System of Next Generation: Potential of a Tubular Flame Burner, Proc. Thermal Engineering Conf., '03 JSME No.03-30, (2003), pp.553–554.

(14) Ishizuka, S., Suzukawa, M., Ishioka, M. and Okada, K., Development of Tubular Flame Burners, Abstracts of WIP Posters, Proc. Combust. Inst., Vol.30 (2004), p.349.

(15) Beer, J.M. and Chigier, N.A., Combustion Aerodynamics, (1972), pp.100–117, Applied Science Publishers Ltd., London.

(16) Syred, N. and Beer, J.M., Combustion in Swirling Flow: a Review, Combust. Flame, Vol.23 (1974), pp.143–201.

(17) Claypole, T.C. and Syred, N., The Effect of Swirl Burner Aerodynamics on NOx Formation, Proc. Combust. Inst., Vol.8 (1981), pp.81–89.

(18) Altgeld, H., Jones, W.P. and Wilhelmi, J., Velocity Measurements in a Confined Swirl Driven Recirculating Flow, Experiments in Fluids, Vol.1 (1983), pp.73–78.

(19) Kobayashi, H. and Kitano, M., Flow Fields and Extinction of Stretched Cylindrical Premixed Flame, Combust. Sci. Technol., Vol.75 (1991), pp.227–239.

(20) Escudier, M.P., Bornstein, J. and Zehnder, N., Observation and LDA Measurements of Confined Turbulent Vortex Flow, J. Fluid Mech., Vol.98 (1980), pp.49–63.

(21) Wunenburger, R., Andreotti, B. and Petitjeans, P., Influence of Precession on Velocity Measurements in a Strong Laboratory Vortex, Experiments in Fluids, Vol.27 (1999), pp.181–188.